



## Magnetohydrodynamic of Copper-Aluminium of Oxide Hybrid Nanoparticles Containing Gyrotactic Microorganisms over a Vertical Cylinder with Suction

Siti Khuzaimah Soid<sup>1,\*</sup>, Afiqah Athirah Durahman<sup>1</sup>, Nur Hazirah Adilla Norzawary<sup>2</sup>, Mohd Rijal Ilias<sup>1</sup>, Amirah Mohamad Sahar<sup>1</sup>

<sup>1</sup> Faculty of Computer and Mathematical Sciences, Universiti Teknologi MARA, 40450 Shah Alam, Selangor, Malaysia

<sup>2</sup> Institute for Mathematical Research (INSPEM), Universiti Putra Malaysia, 43400 Serdang, Selangor, Malaysia

### ABSTRACT

The boundary layer flow with heat and mass transfer are important since the quality of final product depends on factors such as the rate of cooling and stretching phenomenon. The pivotal aim of this research is to address magnetohydrodynamics (MHD) copper-aluminium oxide hybrid nanoparticles containing gyrotactic microorganisms over a stretching vertical cylinder with suction. The mathematical model has been formulated based on Tiwari-Das nanofluid model. Two types of nanofluid containing Copper (Cu) and Aluminum Oxide ( $Al_2O_3$ ) immersed in water is considered in this study. In the analysis, the governing partial differential equations (PDEs) are transformed into a set of ordinary differential equations (ODEs) by a similarity transformation. Corresponding boundary conditions are analysed numerically along with these equations and are programmed in MATLAB software through the *bvp4c* method to obtain the solutions. The numerical solutions are obtained for the skin friction coefficient, the local Nusselt number, local Sherwood number and local density of motile microorganism as well as velocity, temperature, concentration, and microorganism profiles. The present analysis is validated by comparing with previously published work and found to be in good agreement. The effects of the parameter are analysed and discussed. According to the findings, suction increases shear stress, heat transport rate, mass transfer, and mass diffusivity. Moreover, hybrid nanofluid was discovered to be faster than nanofluid in terms of transit rate. Furthermore, the local density motile microorganism bioconvection Peclet number and bioconvection Lewis number increased.

### Keywords:

Magnetohydrodynamic, Gyrotactic  
Microorganisms, Hybrid Nanofluid,  
Suction, Stretching Cylinder

Received: 14 August 2022

Revised: 7 October 2022

Accepted: 10 October 2022

Published: 24 October 2022

## 1. Introduction

In modern industrial and technical practice, boundary layer flow and heat transfer with stretching boundaries have drawn a lot of attention. The characteristics of the ultimate product are heavily reliant on stretching and heat transfer rate during the final step of processing. Because of its practical significance, scientists and engineers have developed an interest in understanding this phenomenon. Extrusion of metals into cooling liquids, food, and plastic items are common examples, as is the

\*Corresponding Author

E-mail address: [khuzaimah@tmsk.uitm.edu.my](mailto:khuzaimah@tmsk.uitm.edu.my)

<https://doi.org/10.37934/araset.28.2.222234>

reprocessing of material in the molten state at high temperatures [1]. Double diffusive convection was studied in a porous medium by Hafizah *et al.*, [1] to enhance the heat transfer. The study of cylinders has recently bought interest among researchers. Mukhopadhyay and Ishak [2] explored the impact of curvature on the skin friction coefficient. They found that when a cylinder is compared to a flat plate, the skin friction coefficient is shown to be higher for the cylinder. Furthermore, as the curvature parameter is increased, the radius of the cylinder shrinks, causing the fluid's motion to accelerate. This is due to the reduced contact surface area of the cylinder with the fluid, which provides less resistance to fluid flow [4]. Additional application regarding cylinder may be found in these literature [5,0].

MHD mixed convective flow along a stretching vertical cylinder has many applications in areas such as heat exchangers, geothermal power generation, nuclear reactors, drilling operations, insulation system and plastic products formation, polymer processing units, etc. Mukhopadhyay [0] stated that heat and mass transfer flow past a stretching surface is mostly investigated. Sharma *et al.*, [0] have investigated heat generation/absorption on MHD mixed convective stagnation point flow in the presence of external magnetic field. Sinha and Yadav [0] did research on steady MHD mixed convection Newtonian fluid flow along a vertical stretching cylinder embedded in porous medium. Lorentz force works as a resistance and retards the fluid motion, due to this resistance some amount of energy transforms into heat and increases the temperature. Further, preliminary investigation by Fatimah *et al.*, [0] on the energy harvesting results in a higher output voltage with the presence of the magnets due to the action of nonlinear magnetic forces.

A hybrid nanofluid is a type of nanofluid that contains two or more different nanoparticles. According to Yang *et al.*, [0] hybrid nanofluid is produced by combining two different types of nanoparticles in the equivalent base fluid to improve thermophysical, optical, rheological, and morphological qualities. Hybrid nanofluids are expected to replace simple nanofluids for a variety of reasons, including a wider absorption range, lower extinction, good thermal conductivity, low pressure-drop, and fewer frictional losses and pumping power when compared to mono nanofluids. Solar collectors, electronic component heat management, machine cutting, engine applications, and automobile cooling have all been tested with hybrid nanofluids. Waini *et al.*, [0] discovered that the heat transfer rate enhanced in the presence of hybrid nanoparticles when compared to standard nanofluid. It has been demonstrated that hybrid nanofluids have greater thermal conductivity than pure nanofluids. Additional hybrid nanofluid references in the direction of MHD may be found in the current literature [12-0].

Microorganisms colonise all ecological niches, including hostile places where few other living things can survive such as the inside engine fuel lines, coal mines and hot springs. Bioconvection happens when microorganisms are swimming in upward direction of fluid and yield instability and amorphous pattern. Due to upward swimming, the gyrotactic microorganisms such as algae tends to concentrate on the upper portion of fluid and produces dense stratification that usually develops wobbly. Bioconvection flows appear in a variety of exciting applications, including environmental systems (ocean algae), fuel cells, and biological polymer synthesis [17]. Hosseinzadeh *et al.*, [0] investigated cross-fluid flow with gyrotactic microorganisms and nanoparticles on a horizontal and three-dimensional cylinder while taking viscous dissipation and magnetic field into account. From the study, the change of bioconvection Lewis number from 0.2 to 0.5, it was observed that the concentration of the microorganisms reduced about 78.38%. We extended Devi and Devi, [0] by adding nanoparticle concentration equation and density of gyrotactic microorganism (bioconvection flow) equation. The pivotal aim of this research is to address  $Cu$  and  $Al_2O_3$  as nanoparticles with water as a base fluid containing gyrotactic microorganism swimming into it with suction and governed by a

boundary layer problem formulation over a stretching vertical cylinder using bvp4c method in MATLAB software.

## 2. Methodology

This study considers a MHD of copper-aluminium oxide hybrid nanoparticles containing gyrotactic microorganisms over a stretching vertical cylinder with suction and a two-dimensional incompressible hybrid nanofluids embedded with water as base fluid through a stretching vertical cylinder. The fluid is a homogeneous mixture of nanoparticles, and gyrotactic microorganisms are also swimming in it. Microorganisms stabilize the suspension of nanoparticles by bio-convective flow which is generated by the combined simultaneous effects of nanoparticles and buoyancy. The linear stretching velocity is denoted by  $U_w(x)$  which is given by  $U_w(x) = U_o x/L$  where reference length,  $L$  and stretching rate,  $U_o$ . The axis of the cylinder is treated along the  $x$ -axis and radial direction along the  $r$ -axis. The externally applied magnetic field,  $B_0$  in the transverse direction is taken. The wall is permeable with  $v_f = -v_0 (v_0 > 0)$ . The viscous and Joule dissipation effects are negligible.

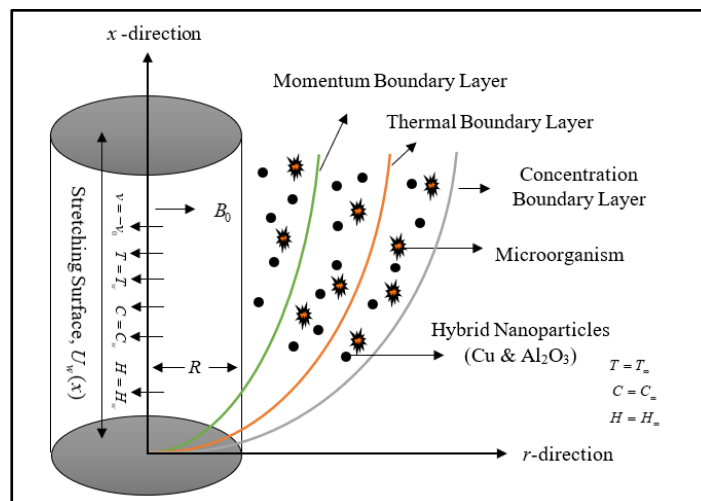


Fig. 1. Physical model of the problem

In this study, two types of nanoparticles used with water as base fluid are considered. The nanoparticles are copper ( $Cu$ ) and aluminium oxide ( $Al_2O_3$ ) termed as  $\phi_1$  and  $\phi_2$  respectively. The equations for evaluating the thermophysical properties of hybrid nanofluids which includes density ( $\rho$ ), heat capacity ( $\rho C_p$ ), dynamic viscosity ( $\mu$ ), thermal conductivity ( $k$ ) and electrical conductivity ( $\sigma$ ) are presented in Table 1 [19]. The thermophysical properties of the base fluid and nanoparticles are presented in Table 2 [19].

**Table 1**  
 Thermophysical Properties of nanoparticles and water 0

Thermophysical properties	Cu ( $\varphi_2$ )	Al <sub>2</sub> O <sub>3</sub> ( $\varphi_1$ )	Water
$\rho$ (kg/m <sup>3</sup> )	8933	3970	997.1
$C_p$ (J/kgK)	385	765	4,179
$k$ (W/mK)	400	40	0.613
$\sigma$ (s/m)	59.6×10 <sup>6</sup>	35×10 <sup>6</sup>	5.5×10 <sup>-6</sup>

**Table 2**  
 Thermophysical Properties of Hybrid Nanofluid 0

Thermophysical properties	Hybrid nanofluid
Density ( $\rho$ )	$\rho_{hnf} = (1 - \varphi_2) [(1 - \varphi_1) \rho_f + \varphi_1 \rho_{y1}] + \varphi_2 \rho_{y2}$
Heat capacity ( $\rho C_p$ )	$(\rho C_p)_{hnf} = (1 - \varphi_2) [(1 - \varphi_1) (\rho C_p)_f + \varphi_1 (\rho C_p)_{y1}] + \varphi_2 (\rho C_p)_{y2}$
Dynamic viscosity ( $\mu$ )	$\mu_{hnf} = \frac{\mu_f}{(1 - \varphi_1)^{2.5} (1 - \varphi_2)^{2.5}}$
Thermal conductivity ( $k$ )	$\frac{k_{hnf}}{k_{bf}} = \frac{k_{y2} + 2k_{bf} - 2\varphi_2 (k_{bf} - k_{y2})}{k_{y2} + 2k_{bf} + \varphi_2 (k_{bf} - k_{y2})}$ <p style="text-align: center;">where</p> $\frac{k_{bf}}{k_f} = \frac{k_{y1} + 2k_f - 2\varphi_1 (k_f - k_{y1})}{k_{y1} + 2k_f + \varphi_1 (k_f - k_{y1})}$
Electrical conductivity ( $\sigma$ )	$\frac{\sigma_{hnf}}{\sigma_{bf}} = \frac{\sigma_{y2} + 2\sigma_{bf} - 2\varphi_2 (\sigma_{bf} - \sigma_{y2})}{\sigma_{y2} + 2\sigma_{bf} + \varphi_2 (\sigma_{bf} - \sigma_{y2})}$ <p style="text-align: center;">where</p> $\frac{\sigma_{bf}}{\sigma_f} = \frac{\sigma_{y1} + 2\sigma_f - 2\varphi_1 (\sigma_f - \sigma_{y1})}{\sigma_{y1} + 2\sigma_f + \varphi_1 (\sigma_f - \sigma_{y1})}$

The subscript 1 and 2 indicate the physical properties of titanium alloy and aluminium alloy respectively. The total volume concentration of both nanoparticles is denoted by  $\varphi$  given as  $\varphi = \varphi_1 + \varphi_2$ .

The governing equations are:

$$\frac{\partial}{\partial x}(ru) + \frac{\partial}{\partial y}(rv) = 0 \tag{1}$$

$$u \frac{\partial u}{\partial x} + v \frac{\partial u}{\partial r} = \left( \frac{\mu_{hnf}}{\rho_{hnf}} \right) \left( \frac{\partial^2 u}{\partial r^2} + \frac{1}{r} \frac{\partial u}{\partial r} \right) - \frac{\sigma_{hnf} B_0^2 u}{\rho_{hnf}} + \frac{1}{\rho_{hnf}} \tag{2}$$

$$\left[ \beta g \rho_f (1 - C_\infty) (T - T_\infty) - g (\rho_n - \rho_f) (C - C_\infty) - g \gamma (\rho_m - \rho_f) (H - H_\infty) \right] = 0$$

$$u \frac{\partial T}{\partial x} + v \frac{\partial T}{\partial r} = \frac{k_{hnf}}{(\rho C_p)_{hnf}} \left( \frac{\partial^2 u}{\partial r^2} + \frac{1}{r} \frac{\partial u}{\partial r} \right) \quad (3)$$

$$u \frac{\partial C}{\partial x} + v \frac{\partial C}{\partial r} = D_B \left( \frac{\partial^2 C}{\partial r^2} + \frac{1}{r} \frac{\partial C}{\partial r} \right) \quad (4)$$

$$u \frac{\partial H}{\partial x} + v \frac{\partial H}{\partial r} + \frac{bw_c}{\Delta C} \left[ \frac{\partial}{\partial r} \left( H \frac{\partial H}{\partial r} \right) \right] = D_M \left( \frac{\partial^2 H}{\partial r^2} + \frac{1}{r} \frac{\partial H}{\partial r} \right) \quad (5)$$

where  $u$  is the component velocity along  $x$ -axis,  $v$  is the component velocity along the  $r$ -axis,  $\nu_{hnf} = \mu_{hnf} / \rho_{hnf}$  is the kinematic viscosity of the hybrid nanofluid,  $\mu_{hnf}$  is the coefficient of fluid viscosity of the hybrid nanofluid,  $\rho_{hnf}$  is the fluid density of hybrid nanofluids,  $g$  is the acceleration due to gravity,  $\beta_{hnf}$  is the coefficient of thermal expansion of the hybrid nanofluid,  $\sigma_{hnf}$  is electrical conductivity of hybrid nanoparticles,  $B_0$  is the strength of magnetic field,  $\beta$  is the thermal expansion coefficient,  $C$  is the concentration of nanoparticles,  $T$  is the fluid temperature,  $k_{hnf}$  is the thermal conductivity of the hybrid nanofluid,  $(\rho C_p)_{hnf}$  is the heat capacity of the hybrid nanofluid,  $\rho_n$  is the density of nanoparticles,  $\rho_m$  is the density of microorganisms particle,  $D_B$  is the diffusivity of nanoparticles,  $H$  is the concentration of microorganisms, and  $D_M$  is the diffusivity of microorganisms,  $b$  is the constant velocity of the plate and  $w_c$  is the maximum cell swimming speed.

The governing equations (1) to (5) are subjected to the boundary conditions given as follows,

$$\begin{aligned} v = v_0, \quad u = U_w, \quad T = T_w, \quad C = C_w, \quad H = H_w \quad \text{at} \quad r = R \\ u \rightarrow 0, \quad T \rightarrow T_\infty, \quad C \rightarrow C_\infty, \quad H \rightarrow H_\infty \quad \text{at} \quad r \rightarrow \infty \end{aligned} \quad (6)$$

Where  $v_0$  is the suction velocity where ( $v_0 > 0$ ),  $U_w$  is the surface stretching velocities,  $T_w$  is the surface temperature,  $C_w$  is the surface concentration,  $H_w$  is the surface microorganism,  $T_\infty$  is the constant ambient temperature.  $C_\infty$  is the constant ambient concentration of nanoparticles and  $H_\infty$  is the constant ambient density of microorganism.

The governing equations which are in the form of partial differential equations (PDEs) are transformed into ordinary differential equations (ODEs) by using similarity transformation method. The similarity variables used are as shown below,

$$\begin{aligned} \eta = \frac{r^2 - R^2}{2R} \sqrt{\frac{U_0}{\nu_f L}}, \quad u = \frac{U_0 x}{L} f'(\eta), \quad v = -\frac{1}{r} \sqrt{\frac{\nu_f U_0}{L}} R f(\eta), \\ \theta(\eta) = \frac{T - T_\infty}{T_w - T_\infty}, \quad \phi(\eta) = \frac{C - C_\infty}{C_w - C_\infty}, \quad \chi(\eta) = \frac{H - H_\infty}{H_w - H_\infty} \end{aligned} \quad (7)$$

where  $\eta$  is the similarity variable,  $\nu_f$  is the kinematic viscosity of the base fluid,  $\theta$  is the dimensionless temperature,  $R$  is the radius of the cylinder,  $L$  is the characteristic length of the cylinder,  $\phi$  is the dimensionless nanoparticle fraction function and  $\chi$  is the dimensionless microorganisms fraction function. By using the similarity variables (7), the PDEs are transformed into ODEs as follows,

$$\varepsilon_1 [(2\eta\kappa + 1)f''' + 2\kappa f''] - [f'^2 - ff''] - \varepsilon_2 \left( \frac{\sigma_{hmf}}{\sigma_f} \right) Mf' + \varepsilon_2 \lambda [\theta - Nr\phi - Rb\chi] = 0 \quad (8)$$

$$\frac{\varepsilon_4}{Pr} \left( \frac{k_{hmf}}{k_f} \right) [(2\eta\kappa + 1)\theta'' + 2\kappa\theta'] + f\theta' = 0 \quad (9)$$

$$f\phi' + \frac{1}{Sc} [(2\eta\kappa + 1)\phi'' + 2\kappa\phi'] = 0 \quad (10)$$

$$(2\eta\kappa + 1)\chi'' + 2\kappa\chi' + (Lb)f\chi' - (Pe) [(2\eta\kappa + 1)(\chi + \omega)\phi'' + ((2\eta\kappa + 1)\chi' + \omega\kappa + \kappa\chi)\phi'] = 0 \quad (11)$$

Along with the boundary conditions,

$$\begin{aligned} f(\eta) = S, \quad f'(\eta) = 1, \quad \theta(\eta) = 1, \quad \phi(\eta) = 1, \quad \chi(\eta) = 1 & \quad \text{at } \eta = 0 \\ f'(\eta) \rightarrow 0, \quad \theta(\eta) \rightarrow 0, \quad \phi(\eta) \rightarrow 0, \quad \chi(\eta) \rightarrow 0 & \quad \text{as } \eta \rightarrow \infty \end{aligned} \quad (12)$$

where  $\varepsilon_1, \varepsilon_2, \varepsilon_3, \varepsilon_4, \varepsilon_5, \varepsilon_6, \varepsilon_7, \varepsilon_8$  and  $\varepsilon_9$  are the thermophysical properties of hybrid nanofluids,  $\kappa = \sqrt{\nu_f L / R^2 U_0}$  is a curvature parameter,  $M = \sigma_f B_0^2 L / \rho_f U_0$  is a magnetic field,  $\lambda = Gr_x / Re_x^2$  is a mixed convection parameter,  $Gr_x = g\beta(1 - C_\infty)(T_w - T_\infty)x^3 / \nu_f^2$  is the Gershoff number,  $Re_x = U_w x / \nu_f$  is a local Reynolds number,  $Nr = (\rho_n - \rho_f)(C_w - C_\infty) / \beta\rho_f(1 - C_\infty)(T_w - T_\infty)$  is buoyancy ratio parameter,  $Rb = \gamma(\rho_m - \rho_f)(H_w - H_\infty) / \beta\rho_f(1 - C_\infty)(T_w - T_\infty)$  is bioconvection Rayleigh number,  $Pr = (\rho C_p)_f \nu_f / k_f$  is a Prandtl number,  $Sc = \nu_f / D_B$  is the Schmidt number,  $Lb = \nu_f / D_M$  is the bioconvection Lewis number,  $Pe = b w_c / D_M$  is the Peclet number and  $\omega = H_\infty / H_w - H_\infty$  is the microorganisms concentration difference parameter, and  $S = \nu_0 / \sqrt{\frac{\nu_f U_0}{L}}$  is a suction.

In this study, physical parameters are skin friction coefficient ( $C_f$ ), local Nusselt number ( $Nu_x$ ), local Sherwood number ( $Sh_x$ ), and local density of motile microorganisms ( $Nn_x$ ) by Khan and Pop [20] are as follows,

$$\begin{aligned} C_f = \frac{\mu_{hmf}}{\rho_f U_w^2} \left( \frac{\partial u}{\partial r} \right) \Big|_{r=R}, \quad Nu_x = -\frac{k_{hmf} x}{k_f (T_w - T_\infty)} \left( \frac{\partial T}{\partial r} \right) \Big|_{r=R}, \quad Sh_x = -\frac{x}{(C_w - C_\infty)} \left( \frac{\partial C}{\partial r} \right) \Big|_{r=R}, \\ Nn_x = -\frac{x}{(H_w - H_\infty)} \left( \frac{\partial H}{\partial r} \right) \Big|_{r=R} \end{aligned} \quad (13)$$

Using the similarity variables (7) where  $Re_x = U_w x / \nu_f$ . Then,

$$\begin{aligned} C_f Re_x^{\frac{1}{2}} = \frac{f''(0)}{(1 - \phi_1)^{2.5} (1 - \phi_2)^{2.5}}, \quad Nu_x Re_x^{-\frac{1}{2}} = -\frac{k_{hmf}}{k_f} \theta'(0), \\ Sh_x Re_x^{-\frac{1}{2}} = -\phi'(0), \quad Nn_x Re_x^{-\frac{1}{2}} = -\chi'(0) \end{aligned} \quad (14)$$

### 3. Results

The transformed governing boundary layer equations are non-linear and are solved numerically by using `bvp4c` in MATLAB. The flow and the heat transfer characteristics are obtained using hybrid nanofluid ( $Cu - Al_2O_3 / water$ ) and nanofluid ( $Cu / water$ ) for the hydromagnetic flow. The effects of velocity, temperature, concentration and microorganisms profiles are illustrated graphically. The effects on the skin friction coefficient  $f''(0)$ , local Nusselt number  $-\theta'(0)$ , local Sherwood number  $-\phi'(0)$  and local Density of Motile Microorganism  $-\chi'(0)$  are tabulated presenting the effects of the physical parameters.

Table 3, 4 and 5 shows the comparison of the skin friction coefficient  $f''(0)$  and the local Nusselt number  $-\theta'(0)$  between the results obtained. Table 3 shown the numerical value of Nusselt number  $-\theta'(0)$  are obtained by comparing the numerical results of present study with W. A. Khan and Pop 0, Devi and Devi 0, and Ahmad *et al.*, 0 which are portrayed in Table 3 in the absence of solid volume fraction  $\phi_1 = 0$  and  $\phi_2 = 0$ , curvature parameter  $\kappa = 0$  for different values of Prandtl number  $Pr$ , and it is noted that our results are found to be in excellent agreement with them.

**Table 3**

Comparison of values of  $-\theta'(0)$  for several values of  $Pr$  when  $\phi_1 = \phi_2 = 0$

$Pr$	W. A. Khan and Pop 0	Devi and Devi 0	Ahmad <i>et al.</i> , 0	Present results
<b>2</b>	0.9113	0.91135	0.91045	0.9113
<b>7</b>	1.8954	1.89540	1.89083	1.8954
<b>20</b>	3.3539	3.35390	3.35271	3.3539
<b>70</b>	6.4621	-	6.47814	6.4622

The numerical value of Skin Friction Coefficient,  $f''(0)$  are obtained by comparing the numerical results of present study with Devi and Devi 0, and Ahmad *et al.*, 0 which are portrayed in Table 4 for  $Cu / water$  (pure nanofluid) in the absence of solid volume fraction  $\phi_1 = 0$  and Table 5 for  $Cu - Al_2O_3 / water$  (hybrid nanofluid) with  $\phi_1 = 0.1$  is fixed throughout the study, curvature parameter  $\kappa = 0$  for different values of  $\phi_2$ , and it is noted that our results are found to be in excellent agreement with them. Therefore, this verifies the reliability and accuracy of the method used for this study.

**Table 4**

Comparison of values of  $f''(0)$  for several values of  $\phi_2$  for  $Cu / water$  (Pure Nanofluid)

$\phi_2$	Devi & Devi 0	Ahmad <i>et al.</i> 0	Present results
<b>0.005</b>	-2.54730	-2.54599	-2.54730
<b>0.02</b>	-2.69147	-2.68993	-2.69147
<b>0.04</b>	-2.88932	-2.88749	-2.88932
<b>0.06</b>	-3.09419	-3.09209	-3.09419

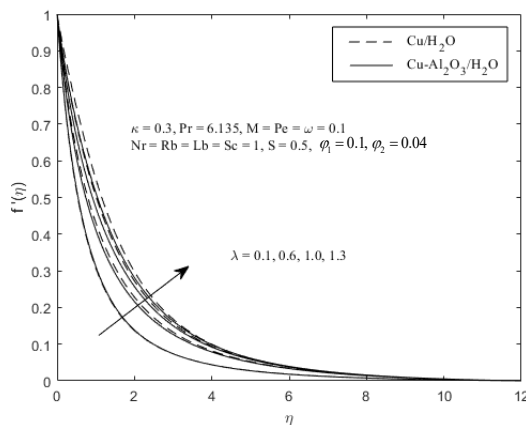
**Table 5**

Comparison of values of  $f''(0)$  for several values of  $\varphi_2$  for  $Cu - Al_2O_3 / \text{water}$  (Hybrid Nanofluid)

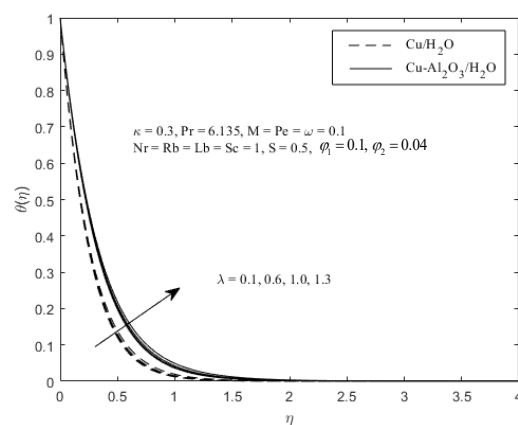
$\varphi_2$	Devi & Devi 0	Ahmad <i>et al.</i> , 0	Present results
<b>0.005</b>	-3.33526	-3.33339	-3.33526
<b>0.02</b>	-3.50377	-3.50168	-3.50377
<b>0.04</b>	-3.73592	-3.73354	-3.73592
<b>0.06</b>	-3.97734	-3.97469	-3.97734

Figure 2 shows the effect for velocity profile when the magnetic increases in the presence of suction. shows the significance of mixed convection parameter  $\lambda$  on the velocity profile  $f'(\eta)$ . Clearly, dimensionless velocity of fluid  $f'(\eta)$  boosts up for growing mixed convective number  $\lambda$ . Larger  $\lambda$  corresponds to an increase in temperature difference leading to enhancement of fluid velocity. For  $\lambda > 0$ , an additional buoyancy induced flow appears. Therefore, fluid velocity enhances and an increment in momentum layer thickness is seen.

Figure 3 shows the effect on temperature profile mixed convection parameter  $\lambda$  increases in the presence of suction. Here distribution profile  $\theta(\eta)$  shows decreasing significance for mixed convection parameter  $\lambda$ . Larger  $\lambda$  leads to an increment in temperature difference which produces decay in temperature profile.



**Fig. 2.** Effects of Velocity profile for various  $\lambda$



**Fig. 3.** Effects of Temperature profile for various  $\lambda$

Concentration profile is presented in Figure 4 for varies values of the mixed convection parameter  $\lambda$ . It has been observed that the concentration of nanoparticles  $f(\eta)$  is depreciated by growing mixed convective number. Higher  $\lambda$  corresponds to an increment in temperature difference which creates reduction in concentration of nanoparticles.

Microorganism profile is presented in Figure 5 for varies values of the mixed convection parameter  $\lambda$  in the presence of suction. For higher values of mixed convective number  $\lambda$ , microorganism field  $\chi(\eta)$  diminishes. Basically, mixed convective number is in direct relation with gravitational acceleration. Therefore, larger estimations of mixed convective number lead to higher gravitational acceleration which shows decay in motile microorganism's concentration.

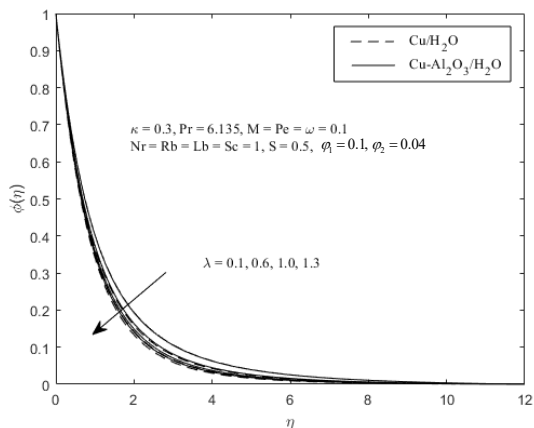


Fig. 4. Effects of Concentration profile for various  $\lambda$

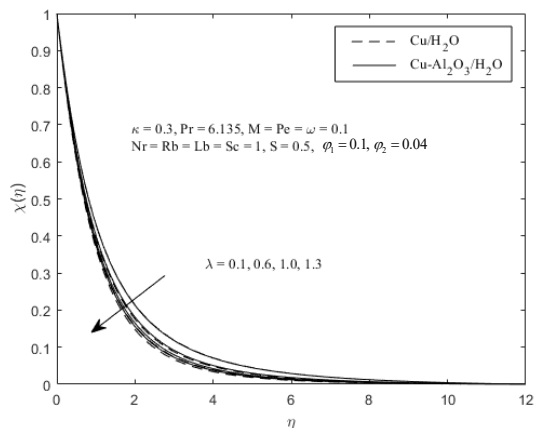


Fig. 5. Effects of Microorganism profile for various  $\lambda$

Figure 6 illustrates the influence of curvature parameter,  $\kappa$  on the temperature profile. When the curvature parameter,  $\kappa = 0$ , it signifies the cylinder's outer surface behaves like a flat surface. Temperature distribution is increasing as the value of curvature parameter,  $\kappa$  increasing. Kelvin temperature has to do with the kinetic energy of molecules and called as the average kinetic energy. When the velocity of the fluid increases, kinetic energy also will increase and cause temperature to increase. It shows that with an increase in  $\kappa$ , the radius of the cylinder decreases which in turn leads to an increase in temperature, near the surface of the cylinder.

Concentration profile is presented in Figure 7 for varies values of the Schmidt number,  $Sc$ . The results present the deceleration of nanoparticle concentration with increasing Schmidt number. The Schmidt number is a fraction of the momentum diffusion rate to the mass diffusion rate. This decrement in the magnitude of nanoparticle concentration is due to the momentum diffusivity increment. This explains about the relation between the concentration of microorganisms and the Schmidt number. The density of the microorganisms decreases with the raising values of the Schmidt number. As Schmidt number increases dynamic viscosity of the fluid increases but the density and mass diffusivity of the nanoparticles decreases hence concentration of the microorganisms decreases.

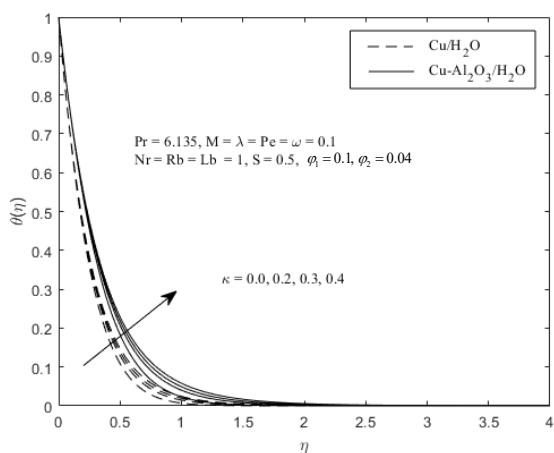


Fig. 6. Effects of Temperature profile for various  $\kappa$

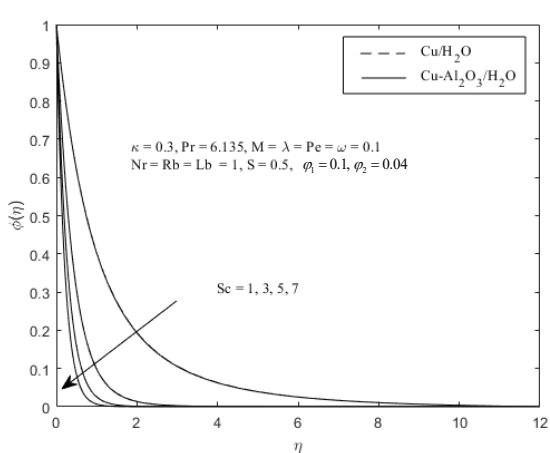


Fig. 7. Effects of Concentration profile for various  $Sc$

Microorganism profile is presented in Figure 8 and 9 for varies values of the bioconvection Lewis number,  $Lb$  and Peclet number,  $Pe$  in the presence of suction. An augmentation in the values of both parameters leads to a less spread of microorganism and physically results a decline of motile boundary layer thickness of nanofluid. The Lewis number causes a decrease in the thickness of the motile microbe layer. This occurs because as the Lewis number grows, so does the viscous diffusion rate, which lowers the velocity distribution at the surface and, as a result, the density of the microorganisms decreases. The bioconvection Peclet number helps in increasing the speed of the microorganisms in relation to the fluid and resulting in a reduction in microbe density at the surface.

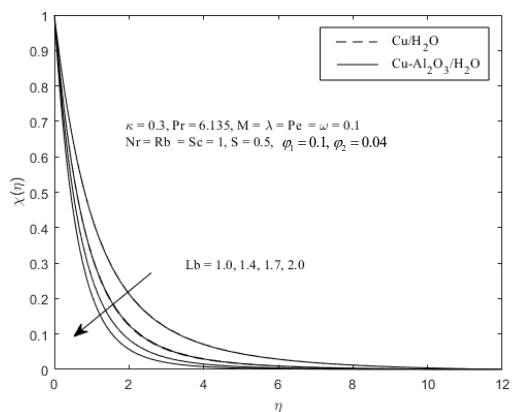


Fig. 8. Effects of Microorganism profile for various  $Lb$

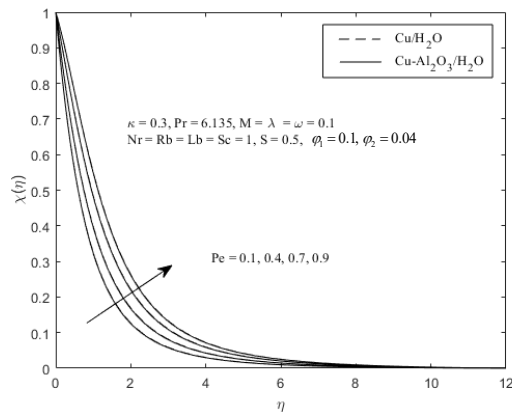


Fig. 9. Effects of Microorganism profile for various  $Pe$

Table 6

Local Sherwood number for  $Cu$  / water and  $Cu - Al_2O_3$  / water

$\varphi_2$	$\lambda$	$M$	$\kappa$	$Sc$	$Lb$	$Pe$	$S$	$-\phi'(0)$	
								$Cu$ / water	$Cu - Al_2O_3$ / water
0.005								1.01458	1.00675
0.02	0.1	0.1	0.3	1	1	0.1	0.5	1.00236	1.00149
0.06	0.1							0.98545	0.99053
	0.1							0.99314	0.99549
0.04	0.6	0.1	0.1	1	1	0.1	0.5	1.05623	1.04699
	1.3							1.10987	1.09311
		0.1						0.99314	0.99549
0.04	0.1	0.5	0.1	1	1	0.1	0.5	0.96646	0.96717
		1.5						0.92089	0.91988
			0.0					0.91731	0.92122
0.04	0.1	0.1	0.2	1	1	0.1	0.5	0.96443	0.96749
			0.4					1.02089	1.02324
				1				0.99314	0.99549
0.04	0.1	0.1	0.3	3	1	0.1	0.5	2.31813	2.32259
				7				4.61921	4.62349
					1.0			0.99314	0.99549
0.04	0.1	0.1	0.3	1	1.4	0.1	0.5	0.98968	0.99276
					2.0			0.98701	0.99066
						0.1		0.99471	0.99741
0.04	0.1	0.1	0.3	1	1	0.4	0.5	0.99299	0.99605
						0.9		0.99075	0.99429
							0.0	0.67199	0.67511
0.04	0.1	0.1	0.3	1	1	0.1	0.5	0.98968	0.99549
							1.5	1.77861	1.78592

The outcomes of local Sherwood number  $-\phi'(0)$  for various variations of involved parameters are tabulated in Tables 6. From Table 6, local Sherwood number increases for higher values of Schmidt number parameter  $Sc$ . Hence, the rate of mass transfer also increases. An upsurge in  $Sc$  is associated to thinner concentration boundary layer. Physically,  $Sc$  connects the relative thickness of the mass transfer layer and the hydrodynamic boundary layer.

#### 4. Conclusions

This present result is extended from the work of Devi and Devi 0 by considering hybrid nanofluid in vertical cylinder and adding term of mixed convection parameter, nanoparticle concentration equation and density of gyrotactic microorganism. The similarity transformation has been used in order to transform the partial differential equation of boundary layer into the form of ordinary differential equation, and then solved by bvp4c solver in MATLAB software. Some of parameters are being considered in this study to determine the behavior of the skin friction coefficient, local Nusselt number, local Sherwood number and local density of motile microorganism, also the velocity, temperature, concentration and microorganism profiles respectively. The results obtained are as follow:

- a. The velocity profile increases when curvature parameter, mixed convection parameter, buoyancy ratio parameter, and bioconvection Rayleigh number increases. However, the profile decreases when volume fraction of Copper, suction, and magnetic field parameter decreases.
- b. The temperature profile increases when volume fraction of Copper, and curvature parameter increases. Furthermore, the profile decreases when suction, and Prandtl parameter decreases.
- c. The concentration profile increases when volume fraction of Copper, and curvature parameter increases. The profile decreases when Schmidt number, and suction decreases.
- d. The microorganism profile increases when volume fraction of Copper, curvature parameter, bioconvection Lewis number, bioconvection Peclet number, and Schmidt number increases. However, the profile decreases when suction, and bioconvection parameter decrease.
- e. The skin friction coefficient increases when volume fraction of Copper, curvature parameter, suction and magnetic field increase. It is decrease when mixed convection parameter, bioconvection ratio parameter, and bioconvection Rayleigh number decrease.
- f. The local Nusselt number increase when volume fraction of Copper, curvature parameter, suction and Prandtl number increase.
- g. The local Sherwood number increase when curvature parameter, and suction increases. Furthermore, it is decrease when volume fraction of Copper and Schmidt number decrease.
- h. The local motile microorganism increases when curvature parameter, suction, bioconvection Lewis number, and bioconvection parameter increase. However, it is decrease when volume fraction of Copper, bioconvection Peclet number, and Schmidt number decreases.

#### Acknowledgement

This research was funded by a grant from Ministry of Higher Education of Malaysia (FRGS/1/2021/STG06/UITM/02/11) and Universiti Teknologi MARA Shah Alam is grateful acknowledged.

## References

- [1] Majeed, Abid, Tariq Javed, and Irfan Mustafa. "Heat transfer analysis of boundary layer flow over hyperbolic stretching cylinder." *Alexandria Engineering Journal* 55, no. 2 (2016): 1333-1339. <https://doi.org/10.1016/j.aej.2016.04.028>
- [2] Abidin, Nurul Hafizah Zainal, Nor Fadzillah Mohd Mokhtar, Izzati Khalidah Khalid, and Siti Nur Aisyah Azeman. "Oscillatory Mode of Darcy-Rayleigh Convection in a Viscoelastic Double Diffusive Binary Fluid Layer Saturated Anisotropic Porous Layer." *Journal of Advanced Research in Numerical Heat Transfer* 10, no. 1 (2022): 8-19.
- [3] Mukhopadhyay, Swati, and Anuar Ishak. "Mixed convection flow along a stretching cylinder in a thermally stratified medium." *Journal of Applied Mathematics* 2012 (2012). <https://doi.org/10.1155/2012/491695>
- [4] Rehman, Khalil Ur, M. Y. Malik, T. Salahuddin, and M. Naseer. "Dual stratified mixed convection flow of Eyring-Powell fluid over an inclined stretching cylinder with heat generation/absorption effect." *AIP Advances* 6, no. 7 (2016): 075112. <https://doi.org/10.1063/1.4959587>
- [5] Ali, Karim M., Mohamed Madbouli, Hany M. Hamouda, and Amr Guaily. "A Stress Mapping Immersed Boundary Method for Viscous Flows." *Journal of Advanced Research in Fluid Mechanics and Thermal Sciences* 87, no. 3 (2021): 1-20. <https://doi.org/10.37934/arfmts.87.3.120>
- [6] Elsayed, Ahmed M. "Design Optimization of Diffuser Augmented Wind Turbine." *CFD Letters* 13, no. 8 (2021): 45-59. <https://doi.org/10.37934/cfdl.13.8.4559>
- [7] Mukhopadhyay, Swati. "MHD boundary layer flow and heat transfer over an exponentially stretching sheet embedded in a thermally stratified medium." *Alexandria Engineering Journal* 52, no. 3 (2013): 259-265. <https://doi.org/10.1016/j.aej.2013.02.003>
- [8] Sharma, P. R., Sharad Sinha, R. S. Yadav, and Anatoly N. Filippov. "MHD mixed convective stagnation point flow along a vertical stretching sheet with heat source/sink." *International Journal of Heat and Mass Transfer* 117 (2018): 780-786. <https://doi.org/10.1016/j.ijheatmasstransfer.2017.10.026>
- [9] Sinha, Sharad, and R. S. Yadav. "STEADY MHD MIXED CONVECTION NEWTONIAN FLUID FLOW ALONG A VERTICAL STRETCHING CYLINDER EMBEDDED IN POROUS MEDIUM." (2021). <https://doi.org/10.29121/ijetmr.v8.i7.2021.990>
- [10] Adnan, Nur Fatimah, Kee Quen Lee, Hooi Siang Kang, Keng Yinn Wong, and Hui Yi Tan. "Preliminary investigation on the energy harvesting of vortex-induced vibration with the use of magnet." *Progress in Energy and Environment* 21 (2022): 1-7. <https://doi.org/10.37934/progee.21.1.17>
- [11] Yang, Liu, Weikai Ji, Mao Mao, and Jia-nan Huang. "An updated review on the properties, fabrication and application of hybrid-nanofluids along with their environmental effects." *Journal of Cleaner Production* 257 (2020): 120408. <https://doi.org/10.1016/j.jclepro.2020.120408>
- [12] Khashi'ie, Najiyah Safwa, Iskandar Waini, Nurul Amira Zainal, Khairum Hamzah, and Abdul Rahman Mohd Kasim. "Hybrid nanofluid flow past a shrinking cylinder with prescribed surface heat flux." *Symmetry* 12, no. 9 (2020): 1493. <https://doi.org/10.3390/sym12091493>
- [13] Teh, Yuan Ying, and Adnan Ashgar. "Three dimensional MHD hybrid nanofluid Flow with rotating stretching/shrinking sheet and Joule heating." *CFD Letters* 13, no. 8 (2021): 1-19. <https://doi.org/10.37934/cfdl.13.8.119>
- [14] Tan, Jian Hong, Toru Yamada, Yutaka Asako, Lit Ken Tan, and Nor Azwadi Che Sidik. "Study of Self Diffusion of Nanoparticle Using Dissipative Particle Dynamics." *Journal of Advanced Research in Numerical Heat Transfer* 10, no. 1 (2022): 1-7.
- [15] Rusdi, Nadia Diana Mohd, Siti Suzilliana Putri Mohamed Isa, Norihan Md Arifin, and Norfifah Bachok. "Thermal Radiation in Nanofluid Penetrable Flow Bounded with Partial Slip Condition." *CFD Letters* 13, no. 8 (2021): 32-44. <https://doi.org/10.37934/cfdl.13.8.3244>
- [16] Vijian, Rashmeera Siva, Mostafa Yusefi, and Kamyar Shameli. "Plant Extract Loaded Sodium Alginate Nanocomposites for Biomedical Applications: A Review." *Journal of Research in Nanoscience and Nanotechnology* 6, no. 1 (2022): 14-30. <https://doi.org/10.37934/jrnn.6.1.1430>
- [17] Das, Kalidas, Pinaki Ranjan Duari, and Prabir Kumar Kundu. "Nanofluid bioconvection in presence of gyrotactic microorganisms and chemical reaction in a porous medium." *Journal of Mechanical Science and Technology* 29, no. 11 (2015): 4841-4849. <https://doi.org/10.1007/s12206-015-1031-z>
- [18] Hosseinzadeh, Kh, So Roghani, A. R. Mogharrebi, A. Asadi, M. Waqas, and D. D. Ganji. "Investigation of cross-fluid flow containing motile gyrotactic microorganisms and nanoparticles over a three-dimensional cylinder." *Alexandria Engineering Journal* 59, no. 5 (2020): 3297-3307. <https://doi.org/10.1016/j.aej.2020.04.037>
- [19] Devi, SP Anjali, and S. Suriya Uma Devi. "Numerical investigation of hydromagnetic hybrid Cu-Al<sub>2</sub>O<sub>3</sub>/water nanofluid flow over a permeable stretching sheet with suction." *International Journal of Nonlinear Sciences and Numerical Simulation* 17, no. 5 (2016): 249-257. <https://doi.org/10.1515/ijnsns-2016-0037>

- [20] Khan, W. A., and I. Pop. "Boundary-layer flow of a nanofluid past a stretching sheet." *International journal of heat and mass transfer* 53, no. 11-12 (2010): 2477-2483. <https://doi.org/10.1016/j.ijheatmasstransfer.2010.01.032>
- [21] Ahmad, Sohail, Kashif Ali, Muhammad Rizwan, and Muhammad Ashraf. "Heat and mass transfer attributes of copper–aluminum oxide hybrid nanoparticles flow through a porous medium." *Case Studies in Thermal Engineering* 25 (2021): 100932. <https://doi.org/10.1016/j.csite.2021.100932>